European Journal of Neuroscience, Vol. 7, pp. 129–142, 1995

Distinct Populations of Identified Glial Cells in the Developing Rat Spinal Cord Slice: Ion Channel Properties and Cell Morphology

Alexandr Chvátal[1], Andrea Pastor[2], Marianne Mauch[3], Eva Syková[1] and Helmut Kettenmann[3]
[1]Laboratory of Cellular Neurophysiology, Institute of Experimental Medicine, Academy of Sciences of the Czech Republic, Vídenská 1083, 142 20 Prague 4, Czech Republic
[2]Max-Delbrück-Centre for Molecular Medicine (MDC), Robert-Rössle-Str. 10, 13122 Berlin, Germany
[3]Institute of Neurobiology, University of Heidelberg, Im Neuenheimer Feld 345, 69120 Heidelberg, Germany

Key words: astrocytes, oligodendrocytes, patch clamp, GFAP, spinal cord

Abstract

Four types of glial cells could be distinguished in the grey matter of rat spinal cord slices at postnatal days 1–19 (P1–P19), based on their pattern of membrane currents as revealed by the whole cell patch clamp technique, and by their morphological and immunocytochemical features. The recorded cells were labelled with Lucifer Yellow, which allowed the subsequent identification of cells using cell-type-specific markers. Astrocytes were identified by positive staining for glial fibrillary acidic protein (GFAP). These were morphologically characterized by multiple, very fine and short processes and electrophysiologically by symmetrical, non-decaying K^+ selective currents. Oligodendrocytes were identified by a typical oligodendrocyte-like morphology, lack of GFAP staining and positive labelling with a combination of O1 and O4 antibodies (markers of the oligodendrocyte lineage), and their membrane was dominated by symmetrical, passive, decaying K^+ currents. The third population of glial cells was also characterized by positive staining for O1/O4 or only for O4 antigens, lack of GFAP staining and, in some cells, oligodendrocyte-like morphology. However, these cells could be distinguished by the presence of inwardly rectifying (K_{IR}), delayed outwardly rectifying (K_{DR}) and A-type K^+ currents (K_A), representing the most likely glial precursor cells of the oligodendrocyte lineage. The fourth population of glial cells had small somata and a widespread network of long processes with no apparent orientation preference. In one case, processes were positively labelled with GFAP, while 30% were characterized by faint, diffuse staining. These cells expressed a complex pattern of voltage-gated channels, namely Na^+, K_{DR}, K_A and K_{IR} channels. In contrast to neurons, the amplitude of Na^+ currents was at least one order of magnitude smaller than the K^+ currents, and none of these cells showed the ability to generate action potentials in the current clamp mode. Since none of these cells could be labelled by oligodendrocyte markers we assume that they were either astrocytes or glial precursor cells of the astrocyte lineage. The four cell types were found in all regions of the grey matter. When randomly accessing the glial cells, the probability of recording from the oligodendrocyte precursor cells and the glial cells with Na^+ currents decreased during development. At P1–P3, 50% of the cells revealed the Na^+ current, while at P13–P15 only 18% did. Concomitantly, the number of glial cells with astrocyte- and oligodendrocyte-like membrane currents increased from 19 and 12% to 41 and 35.5% respectively. We conclude that the glial cells in the spinal cord slices possess distinct morphological, immunohistochemical and physiological properties, and that the glial populations undergo changes during postnatal development.

Introduction

Glial cells can express a variety of voltage-gated channels, including K^+, Na^+ and Ca^{2+} channels (Ritchie, 1992; Barres *et al.*, 1990a; MacVicar, 1984). Studies have shown that there are marked differences between oligodendrocytes, astrocytes, glial precursor cells and microglial cells (Barres *et al.*, 1988; Kettenmann *et al.*, 1992, 1993). So far most of these studies have been performed in tissue culture and little information is available yet on the presence of these channels *in situ*. One way to avoid cell culture artefacts is to isolate glial cells from brain tissue. Thus the membrane properties of optic nerve and hippocampal glial cells have been described (Barres *et al.*, 1990b; Tse *et al.*, 1992). By applying the patch-clamp technique to thin brain slices (Edwards *et al.*, 1989) it has become possible to access glial cells in their normal cellular environment and to re-evaluate the results obtained in tissue culture. Furthermore, the brain slices permit

Correspondence to: H. Kettenmann at Max-Delbrück-Centre for Molecular Medicine

Received 19 November 1993, revised 26 January 1994, accepted 13 July 1994

the study of glial cells during development, since slices from animals of different postnatal ages can be compared.

In a corpus callosum slice preparation it was possible to determine the changes in channel expression pattern during the development of oligodendrocytes from their precursors (Berger *et al.*, 1991). Berger *et al.* (1991, 1992a, b) demonstrated that there is a marked change in the channel pattern at the time when the precursor cell differentiates to an oligodendrocyte. This process is highly synchronized at a defined age of the animal; for example, at postnatal day 3 (P3), P8 or P26 most glial cells have uniform membrane properties. In contrast, a study from the grey matter of the mouse hippocampal slice at about P10 revealed that even in the restricted region of CA1 several populations of glial cells could be distinguished based on their electrophysiological properties (Steinhäuser *et al.*, 1992). The cells were identified as glial based on their ultrastructural features as resolved under the electron microscope, but were not further identified as being astrocytes, oligodendrocytes or glial precursor cells. Recently, expression of voltage-activated K^+ channels by astrocytes and oligodendrocytes was described in hippocampal slices of rats at P5–P24 (Sontheimer and Waxman, 1993). These authors found voltage-activated Na^+ currents in 11 out of 105 cells, but only five cells were identified immunocytochemically as astrocytes by positive glial fibrillary acid protein (GFAP)-staining and none as oligodendrocytes.

In the present study we have applied the slice technique to study glial cells in their natural environment in the grey matter of the rat spinal cord. We used slices from P1 to P19 since gliogenesis in the rat spinal cord occurs in the first three postnatal weeks (Gilmore, 1971; Matthews and Duncan, 1971; Sims *et al.*, 1985; Hirano and Goldman, 1988). It is evident that glial cells play an important role in extracellular ionic and volume homeostasis (for reviews see Syková, 1983, 1992; Walz, 1989; Chelser, 1990). However, the regulatory processes controlling K^+, pH and extracellular volume homeostasis in the spinal cord are not operative in the first postnatal week but develop in parallel with the differentiation of the glial cells (Jendelová and Syková, 1991). The importance of glial cells for ion homeostasis is further supported by the observation that an impairment of gliogenesis, e.g. by early postnatal X-irradiation (Gilmore, 1963), prevents the development of the regulatory processes which contribute to ion homeostasis (Syková *et al.*, 1992). During postnatal development the extracellular space volume shrinks to half its original size during the first two postnatal weeks (Lehmenkühler *et al.*, 1993; Syková and Chvátal, 1993) and therefore the microenvironment of the neurons and glial cells changes. We have recently demonstrated that the changes in electrophysiological properties of oligodendrocytes in the corpus callosum coincide with the decrease in the extracellular volume (Syková *et al.*, 1994). To understand these complex events, the basic properties of glial cells have to be understood during this critical developmental period.

So far, the membrane properties of astrocytes and oligodendrocytes from spinal cord have been studied only in culture (Kettenmann *et al.*, 1983; Sontheimer and Kettenmann, 1988; Sontheimer *et al.*, 1992). The studies revealed that astrocytes in spinal cord express a number of voltage-gated channels and that their expression can be modulated by the presence of neurons (Sontheimer and Waxman, 1992; Sontheimer *et al.*, 1992; Thio *et al.*, 1993). It has also been shown that oligodendrocytes express time-independent K^+ channels (Kettenmann *et al.*, 1982, 1984).

In the present study on spinal cord slices from rats at P1–P19 we demonstrate that there are four histologically and/or electrophysiologically distinct glial cell populations in the grey matter of the spinal cord. They are identified as astrocytes, oligodendrocytes and precursor cells. Moreover, we demonstrate that the relative proportions of these populations change with development.

Materials and methods

Preparation of spinal cord slices and electrophysiological set-up

Young rats were killed at P1–P19 by decapitation. The spinal cords were quickly dissected out and washed in artificial cerebrospinal solution at 8–10°C. A 3–4 mm long segment of the spinal cord was embedded in 1.7% agar (Difco, Detroit, MI). The spinal cord was cut transversally into 120–150 μm thick slices using a vibratome (FTB; Plano, Marburg, Germany). Slices were transferred to a nylon net in cold (5°C) bathing solution and were then slowly warmed up to room temperature. For electrophysiological recordings, slices were placed in a chamber mounted on the stage of a Zeiss microscope (modified Standard 16; Zeiss, Oberkochen, Germany) and fixed in a chamber using a U-shaped platinum wire with a grid of nylon threads (Edwards *et al.*, 1989). The chamber was continuously perfused with oxygenated bathing solution and substances were added by changing the perfusate. Cell somata in the spinal cord slice were visible in normal water immersion optics and could be approached by the patch electrode. The image was detected with an infrared-sensitive video camera (C3077; Hamamatsu Photonics, Hamamatsu City, Japan) and displayed on a standard black-and-white monitor.

The selected cells had a clear, dark membrane surface and were located 10–30 μm beyond the surface of the slice. Positive pressure was applied to the recording pipette while it was lowered to the slice under microscope control. The cellular debris was blown aside so that the tip could be placed onto the surface of a cell soma. Membrane currents were measured with the patch-clamp technique on the whole-cell recording configuration (Hamill *et al.*, 1981). Current signals were amplified with conventional electronics (EPC-7 amplifier; List Electronics, Darmstadt, Germany), filtered at 3 kHz and sampled at 5 kHz by an interface (TIDA; Battelle Europe, Frankfurt, Germany) connected to an AT-compatible computer system which also served as a stimulus generator.

Solutions and electrodes

Standard bathing solution was used in our experiments with the following composition (in mM): NaCl 134.0, KCl 2.5, $CaCl_2$ 2.0, $MgCl_2$ 1.3, K_2HPO_4 1.25, $NaHCO_3$ 26.0, D-glucose 10.0, pH 7.4 (the total K^+ concentration was thus 5 mM). The solution was gassed with a mixture of 95% O_2 and 5% CO_2. In solutions with increased concentration of K^+, NaCl was replaced by equimolar KCl. The internal pipette solution had the following composition (in mM): KCl 130.0, $CaCl_2$ 0.5, $MgCl_2$ 2.0, EGTA 5.0, HEPES 10.0, pH 7.2. All experiments were carried out at room temperature (~22°C). Recording pipettes were fabricated from borosilicate capillaries (Hilgenberg, Malsfeld, Germany) and coated with Sigmacote (Sigma, Taufkirchen, FRG). The open resistance of these patch pipettes was 5–6 MΩ. The pipette always contained 1 mg/ml Lucifer Yellow (Fluka, Buchs, Switzerland).

Intracellular staining of cells

During recording, cells were filled with Lucifer Yellow by dialysing the cytoplasm with the patch pipette solution. To avoid destruction of the cell through pulling off the pipette after recording, we destroyed the seal by injection of a large hyperpolarizing current. After recording from the cell, the slice was fixed for 3–5 h at room temperature in

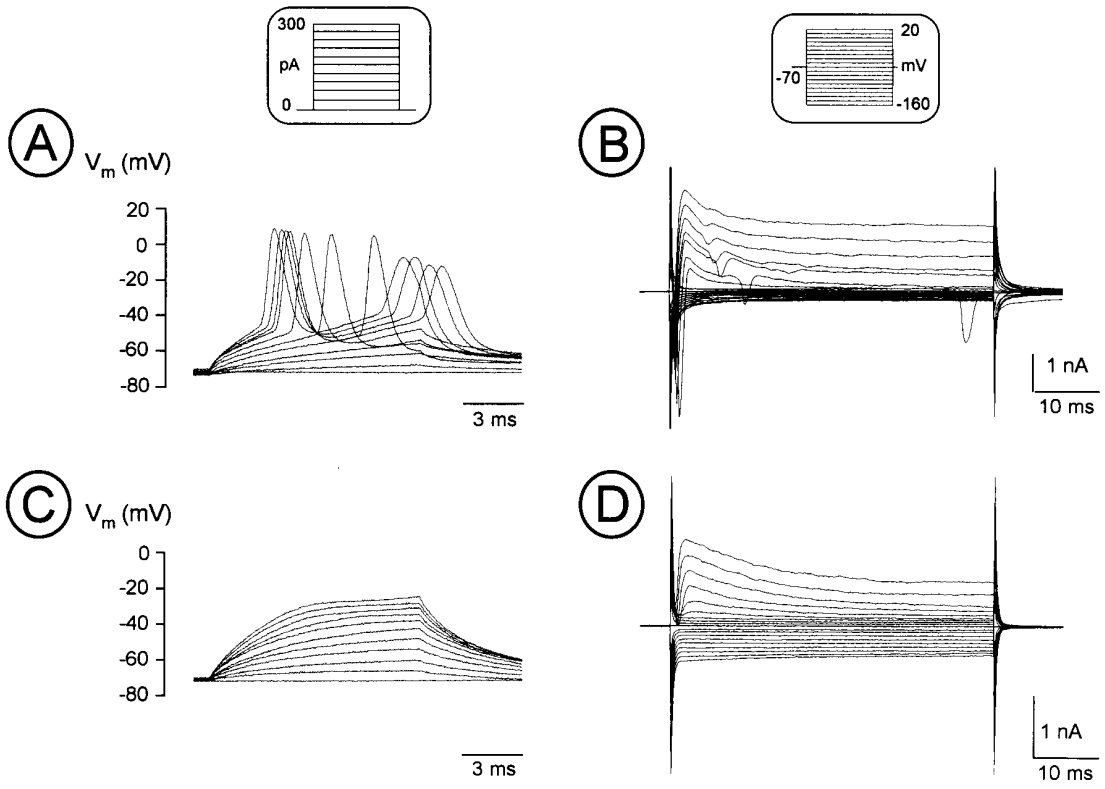

FIG. 1. Responses of glial cells and neurons to depolarization. (A) In the current-clamp mode depolarizing current pulses with increasing amplitude were injected into a cell from P5. The pattern of current pulses is illustrated in the inset above. These depolarizations elicited action potentials. (B) In the voltage-clamp mode, current recordings from the same cell illustrate the large transient inward current activated by depolarization. The pattern of voltage-clamp commands is illustrated in the inset above. Recordings identified the cell as a neuron. The resting membrane potential was –70 mV. (C) A similar protocol was used to identify a glial cell. No active voltage responses were recorded in the current-clamp mode. (D) In the voltage-clamp mode a small inward current is activated with depolarization. The resting membrane potential was –67 mV; the cell is from P5.

4% paraformaldehyde in 0.1M phosphate buffer, pH 7.4. Slices were then transferred to phosphate buffer. Lucifer Yellow-filled cells were examined in a fluorescence microscope equipped with a fluorescein isothiocyanate filter combination (band pass 450–490 nm, mirror 510 nm, long pass 520 nm).

Immunocytochemistry

Indirect immunofluorescence was performed on spinal cord slices after electrophysiological recording and injection of Lucifer Yellow. Monoclonal antibodies O1 and O4, characterized by Sommer and Schachner (1981), and antibodies to GFAP (Eng *et al.*, 1971; Debus *et al.*, 1983; and monoclonal mouse-anti-GFAP, Böhringer, Mannheim) were used in this study to identify oligodendrocytes and astrocytes, respectively. The binding of O1 and O4 antibodies was visualized with goat anti-mouse immunoglobulin antibodies coupled to Texas Red and GFAP either with swine anti-rabbit immunoglobulin antibodies coupled to rhodamine, or with goat anti-mouse immunoglobulin antibodies coupled to Cy3.

Results

Identification of glial cells

The measurements were carried out on 260 glial cells in the grey matter of spinal cord slices between P1 and P19. To access glial cells, we approached cell somata with a small diameter. After formation of the whole-cell recording configuration, we used two protocols to distinguish these cells from neurons. Firstly, glial cells were identified as cells in which current pulses of up to 480 pA depolarized the cells up to 70 mV and did not activate action potentials in the current clamp mode (Fig. 1C). Moreover, no spontaneous electrical activity was observed. In contrast, neurons were identified by their ability to generate action potentials.

In the voltage-clamp mode, membrane currents were activated by clamping the membrane from the holding potential of –70 mV to values ranging from 20 to –160 mV. Depolarization elicited large, transient inward currents in the neuronal population due to the activation of Na^+ channels but produced none or only small currents in the glial cells. The pulse protocol distinguished four main types of glial cells (with apparent subtypes, which were not analysed in detail) based on their distinct membrane current pattern (see below). Electrophysiologically characterized cells were dialysed and thereby filled with Lucifer Yellow. By this procedure we studied both the membrane currents and the morphology of a distinct glial cell.

To identify the electrophysiologically characterized cells, we stained the slices with antibodies to GFAP (n = 46), with a combination of antibodies to O1 and O4 (O1/O4) (n = 26) or with O4 alone (n = 9) after recording and injection of cells with Lucifer Yellow. These antibodies recognize astrocytes (GFAP) and cells of the oligodendrocyte lineage (O1/O4, O4).

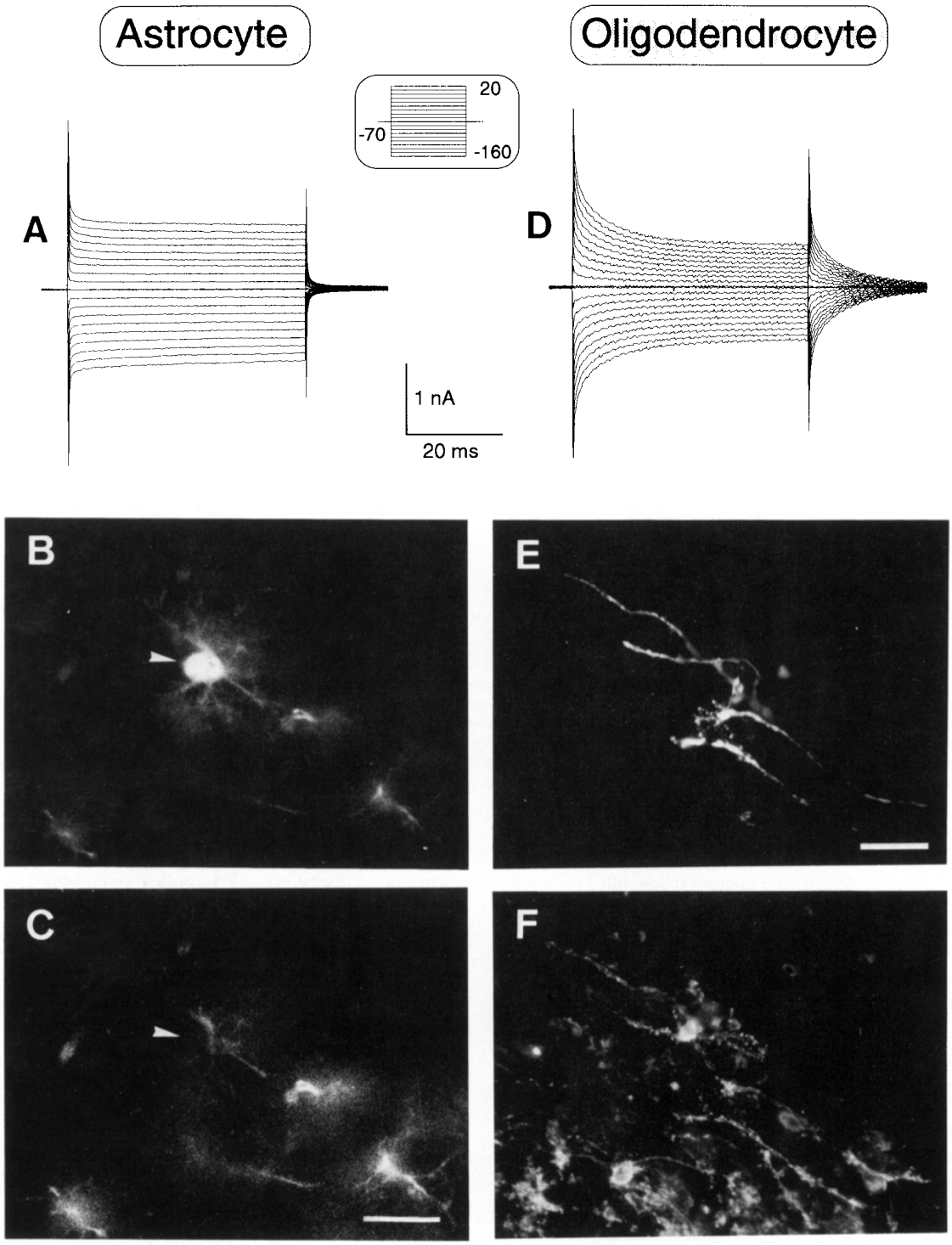

FIG. 2. Membrane current pattern and morphology of identified astrocytes and oligodendrocytes in rat spinal cord. Membrane currents were recorded while the membrane potential was clamped at –70 mV. To activate voltage-gated currents, the membrane was clamped for 50 ms to increasing de- and hyperpolarizing potentials (pattern of voltage commands see inset in the upper middle) ranging from –160 to 20 mV, with 10 mV increments. Current traces are not corrected for leakage and capacitance currents. (A) In this cell from P7, the de- and hyperpolarizing voltage jumps resulted in symmetrical currents with no apparent time-dependence. The resting potential was –76 mV. During the recording the cell was filled with Lucifer Yellow which is shown in (B). This cell was identified as an astrocyte by a positive staining for GFAP, as shown in (C). (D) The current pattern of a cell from P5 shows symmetrical, slowly decaying inward and outward currents. The resting potential was –71 mV. The Lucifer Yellow-filled cell is depicted in (E). (F) The same cell as in (D) and (E) is identified as an oligodendrocyte by a positive staining for O1/O4. Scale bars: (B), (C): 20 μm; (E), (D): 10 μm.

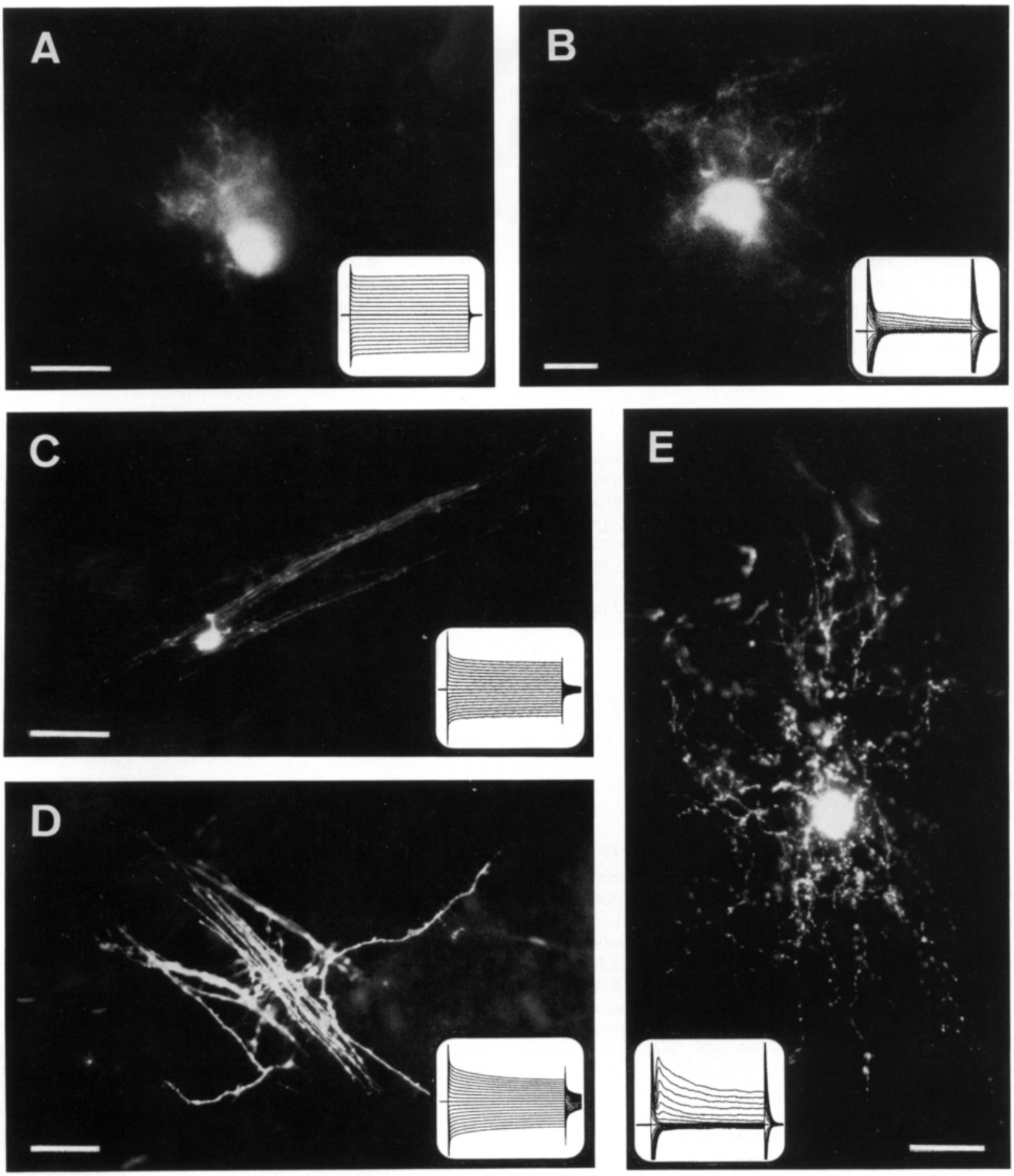

FIG. 3. Morphology of Lucifer Yellow injected glial cells. Glial cells were filled with Lucifer Yellow via the patch pipette and inspected in the fluorescence microscope. The photomicrographs show an astrocyte from P8 (A), two oligodendrocytes from P11 and P10 (C and D), an oligodendrocyte precursor from P5 (B) and a glial cell with Na^+ current from P5 (E). The corresponding current pattern was obtained as described in the legend to Fig. 2 and is illustrated in the insets. Scale bars: (A), (B) and (E), 20 μm; (C) and (D), 40 μm. Note that due to the intense fluorescence of the soma in comparison to the processes, the somatic diameter appears much larger as seen in the infrared optics.

Astrocytres have symmetrical, non-decaying K^+ currents

In 44 cells depolarizing and hyperpolarizing voltage steps activated symmetrical outward and inward currents respectively, with no apparent decay during the voltage step (Fig. 2A). Six of the cells were positively identified as astrocytes by GFAP staining (Fig. 2C). Fourteen cells were GFAP-negative, but were physiologically indistinguishable from the GFAP-positive cells. The cells were characterized by round cell bodies of 8–10 μm in diameter with short, very fine processes which formed a diffuse network around the cell (Figs 2B and 3A). It should be noted that the values for the somatic diameter were obtained with infrared optics. The image of the Lucifer Yellow fluorescence, as shown in the figures, gives the impression of a larger somatic diameter (Figs 2 and 3). This is due to the high fluorescence of the soma compared with the processes, which leads to an overexposure of the film. In one out of 44 cases we observed dye coupling to another cell (P5).

The resting membrane potential (V_r) of these cells was -69.4 ± 7.7 mV (mean ± SD). To identify the ionic species of the currents, the K^+ gradient across the membrane was changed by increasing K^+ concentration in the bathing solution from 5 to 55 mM. Superfusion of the cell with 55 mM K^+ evoked an inward current. The depolarizing steps from the holding potential (–70 mV) to –35, 0 and 35 mV and hyperpolarizing steps to –105 and –140 mV showed that the inward and outward conductance increased. The reversal potential of the currents shifted from –70 mV in 5 mM K^+ (K^+ equilibrium potential –83 mV) to –16 mV in 55 mM K^+ (K^+ equilibrium potential –23 mV), thus following the K^+ equilibrium potential ($n = 3$). Application of Ba^{2+} blocked the currents by 28–71% ($n = 4$) in cells from P3–P7 and by 3–27% ($n = 5$) in cells from P11–P12.

We tested for the presence of A-type K^+ currents (K_A currents) by applying increasing depolarizing voltage steps, starting from two holding potentials, –70 and –110 mV. When subtracting these, two families of current traces K_A currents can be isolated (Connor and Stevens, 1971). With one exception K_A currents were not detected in immunohistochemically ($n = 6$) and electrophysiologically identified astrocytes ($n = 15$).

Oligodendrocytes have symmetrical, decaying K^+ currents

Sixty-one cells expressed symmetrical currents which decayed during the voltage step (Fig. 2D), as previously described for oligodendrocytes in the corpus callosum (Berger *et al.*, 1991). The cells were identified as cells of the oligodendrocyte lineage by positive staining with O1/O4 antibodies (9 out of 18 cells) and the lack of GFAP staining ($n = 8$). Oligodendrocytes had a round cell body of ~10–15 μm diameter with very long processes, which were usually oriented in parallel to each other (Figs 2E and 3C, D). In five cases out of 61, these cells were dye coupled to other cells. Coupling was observed at P4 (1 cell), P5 (1 cell), P9 (2 cells) and P11 (1 cell).

The currents decayed with a time constant which varied between 5 and 20 ms among the cells tested. For one given cell the time constant of decay was voltage-independent. After the offset of the depolarizing or hyperpolarizing voltage step symmetrical inward and outward tail currents appeared which were not observed in astrocytes (Figs 2 and 4). The tail currents decayed with a similar time constant as the currents evoked by the voltage step. The V_r of these cells was -65.2 ± 9.4 mV.

Superfusion of oligodendrocytes with 55 mM K^+ evoked similar inward currents and a shift in the current reversal potentials as described for astrocytes, thus identifying this current as a K^+ current ($n = 3$). Application of Ba^{2+} blocked the decaying component of the K^+ current by 13–35% ($n = 5$) at P3–P7 and by 8–48% ($n = 6$) in cells from P11–P12. In contrast to the astrocytes, the tail currents were blocked in the presence of Ba^{2+} (Fig. 4). Na^+ or K_A currents were not detected in immunohistochemically ($n = 9$) and morphologically identified oligodendrocytes ($n = 11$) using the protocol as described above.

Precursor cells of the oligodendrocyte lineage express voltage-gated K^+ currents

The third population of cells ($n = 62$) was characterized by delayed rectifying K^+ (K_{DR}) and K_A currents at positive potentials. Seventy-nine per cent of the cells also displayed inwardly rectifying K^+ (K_{IR}) currents at negative potentials (Fig. 5A). The V_r of the cells with a K_{IR} was -65.4 ± 8.8 mV ($n = 49$), whereas the V_r of cells without K_{IR} was -48.9 ± 10.8 mV ($n = 13$). Three out of 11 cells were identified as cells of the oligodendrocyte lineage by positive staining for the O1/O4 ($n = 1$) or for O4 only ($n = 2$) antigens (Fig. 5C). The positively identified cells had some processes oriented in parallel, but these were not as long as in oligodendrocytes with passive decaying currents (Figs 3B and 5B). All tested cells were negative for GFAP ($n = 4$).

Time-independent small outward currents were recorded for voltage jumps to –60 and –50 mV (from a holding potential of –70 mV). With further depolarization (–40 mV) a slowly activating additional current component was observed. This current component could be isolated by subtracting the small, time-independent current recorded at –50 mV multiplied by the relative potential jump (Fig. 6A). For instance, to resolve the K_{DR} current at –20 mV (jumping from the holding potential of –70 mV), the current in response to the voltage jump from –70 to –50 mV was multiplied by 2.5 and subtracted. The resulting family of current traces showed properties of a K_{DR} current (Fig. 6A).

The K_{IR} currents elicited in 79% of the cells inactivated at potentials more negative than –120 mV. This K_{IR} current was separated from the time-independent current using a similar protocol as described for the isolation of the K_{DR} current (Fig. 6A). Superfusion of these oligodendrocyte precursor cells with 55 mM K^+ resulted in a shift of the current reversal potential of the K_{DR} current as expected for a K^+ selective conductance. Application of Ba^{2+} only partially blocked the outward current by $45 \pm 11\%$ ($n = 6$). The K_{IR} current was completely blocked (not shown).

The current protocol to isolate K_A currents described above revealed the presence of this current type (Fig. 6B). K_A currents were activated at potentials more positive than –60 mV and decayed with a time constant ranging between 10 and 70 ms (for a voltage jump to 20 mV). These immunohistochemically, morphologically and electrophysiologically distinct cells characterized by K_{DR}, K_A and K_{IR} channels (see Table 1) have properties as described for cultured glial precursor cells of the oligodendrocyte lineage (Sontheimer *et al.*, 1989).

Glial cells with voltage-gated K^+ and Na^+ currents

In the fourth group of cells ($n = 93$) depolarizing voltage steps to potentials less negative than –40 mV activated outward currents which slowly inactivated during the voltage step (Fig. 5D). The inactivation is mainly evoked by the K_A current, which is partially active at a holding potential of –70 mV. If the holding potential was –50 mV, the outward currents showed a considerably smaller inactivating component (Fig. 7, left column). Depolarization to potentials less negative than –50 mV activated an additional current component, namely a transient inward current which preceded the K_{DR} current.

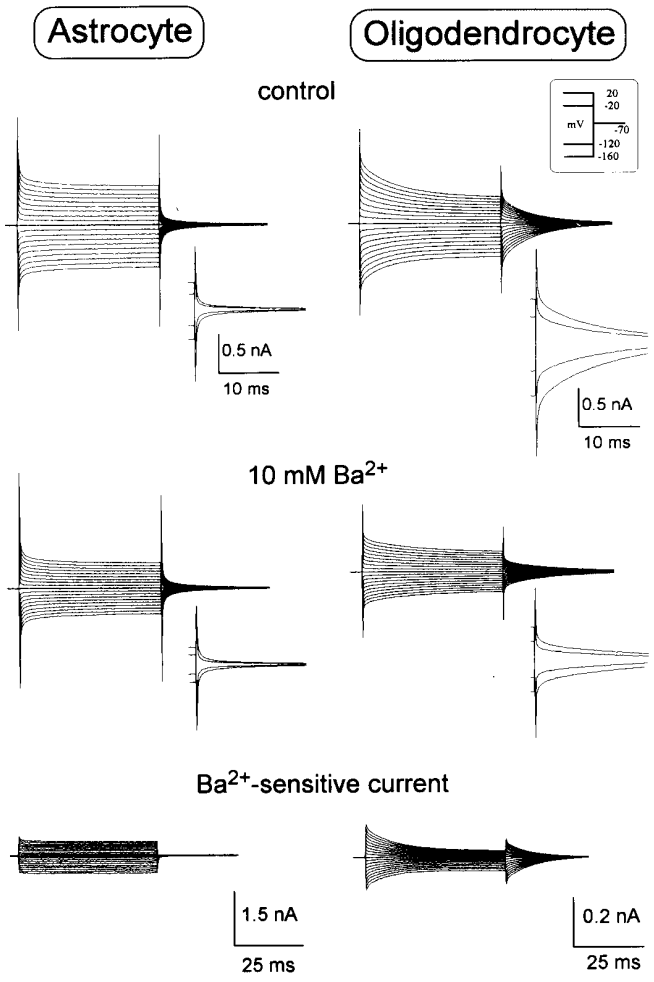

FIG. 4. Ba^{2+} sensitivity of tail current in astrocytes and oligodendrocytes. The effect of extracellularly applied Ba^{2+} (10 mM) on membrane currents of astrocytes and oligodendrocytes was investigated. The pattern of voltage steps was as described in the legend to Figure 2. In both cell types the membrane currents activated with de- and hyperpolarizing voltage steps were partially blocked by Ba^{2+}. In astrocytes (left column) the size of the tail currents did not apparently change in Ba^{2+}, whereas in oligodendrocytes (right column) a remarkable block of the tail currents was induced. (Compare enlarged tail currents under control conditions and in the presence of Ba^{2+} on the bottom; the Ba^{2+}-sensitive current was obtained by subtracting currents in Ba^{2+} from currents recorded under control conditions.)

Hyperpolarizing voltage steps elicited a K_{IR} current in 54 out of 93 cells (58% of all cells), which was similar to that described for the oligodendrocyte precursor cells. In the remaining 39 cells only a very small, time-independent inward current was observed. The V_r of the cells with K_{IR} was –61 ± 12.7 mV (n = 54), whereas the cells without K_{IR} showed a less negative V_r of –51 ± 14.4 mV (n = 39). Ten out of 14 cells were GFAP-negative. In one cell some processes were labelled with the typical filamentous GFAP-staining pattern (Fig. 5F). In three other cells a faint, diffuse staining was observed. In contrast, stainings with the O1/O4 antibodies were always negative (n = 5). The cells were characterized by small cell bodies (~5–10 µm in diameter), a widespread network of long processes with no apparent orientation preference (Figs 3E and 5E) and no dye coupling to other cells.

Superfusion of these cells with 55 mM K^+ in the bathing solution had a marked effect on the K_{DR} current. When comparing the current voltage relation determined 60 ms after the voltage jump (when the rapid transient current was completely inactivated) in normal and elevated K^+ concentrations, the reversal potential was close to the K^+ equilibrium potential (Fig. 8A). The current protocol to isolate K_A currents revealed the presence of K_A channels (Fig. 9A). Application of Ba^{2+} partially blocked the K_{DR} and K_{IR} currents (block by 53.8 ± 16%, n = 12; Fig. 8B) whereas TEA (50 mM) and 4-AP (5 mM) mainly blocked the K_{DR} and K_A currents (Fig. 7). TEA blocked the K_{DR} current by 28 ± 16% (n = 4) and the K_A current by 29.5 ± 13% (n = 4) respectively. The K_{IR} current was not apparently reduced in the presence of TEA (n = 4). 4-AP blocked the K_{DR} current by 36.8 ± 19% (n = 5) and the K_A current by 52.1 ± 7% (n = 5), whereas the K_{IR} current was only blocked by 9.2 ± 10% (n = 5).

These cells were distinguished by the presence of fast transient inward currents ranging from 20 to 550 pA; this current component was not observed in Na^+-free bathing solution, identifying it as a Na^+ current. Figure 9B shows the net inward current obtained by subtracting currents in Na^+-free solution from currents in standard bathing solution. This inward current activated within 1–2 ms and inactivated within 3–5 ms. The current voltage relation revealed a peak between –20 and +20 mV (n = 39) and the extrapolated reversal potential was at ~75–80 mV, i.e. close to the Na^+ equilibrium potential.

Changes of the glial populations during development

When randomly accessing the glial cells, the relative number of cells with Na^+ currents gradually decreased from P1–P3 to P13–P15 from 50 to 18%. Similarly, there was a lower probablity of recording in glial cells with voltage-gated K^+ currents (and no Na^+ currents), the oligodendrocyte precursor cells, in older (P13–P15) slices (6%) than in younger (P1–P3) (19%). In contrast, the number of astrocytes and oligodendrocytes with passive K^+ currents increased from 19 and 12% to 41 and 35.5% respectively (Fig. 10). None of the four cell types was confined to a specific region of the spinal cord grey matter either in early postnatal days (at P1–P5) or later (at P10–P19).

Discussion

Identification of glial cells

In this study we have recorded membrane currents of glial cells in the grey matter of the rat spinal cord. We could distinguish these cells from neurons based on physiological and immunocytochemical data. These features are summarized in Table 1. Glial cells either did not show any Na^+ currents, or the Na^+ current was much too small to generate action potentials. Among these glial cells we could distinguish between four types based on their pattern of membrane currents and immunohistochemical and morphological features. Six out of 20 cells characterized by passive non-decaying currents were positive for GFAP, thus identifying these cells as astrocytes. The finding that cells with an identical current pattern can be both GFAP-negative and -positive is not surprising, since astrocytes, in particular in an immature state, may not express GFAP (Fischer *et al.*, 1982; Levison and Goldman, 1993).

The second type of GFAP-positive cells was distinguished by the presence of Na^+ currents and was characterized by a complex pattern of voltage-gated channels similar to those described in early precursor cells in cortical cultures or corpus callosum slices (Berger *et al.*, 1991). We could, however, only identify one cell with distinct fibrillary GFAP staining and three others with more faint labelling.

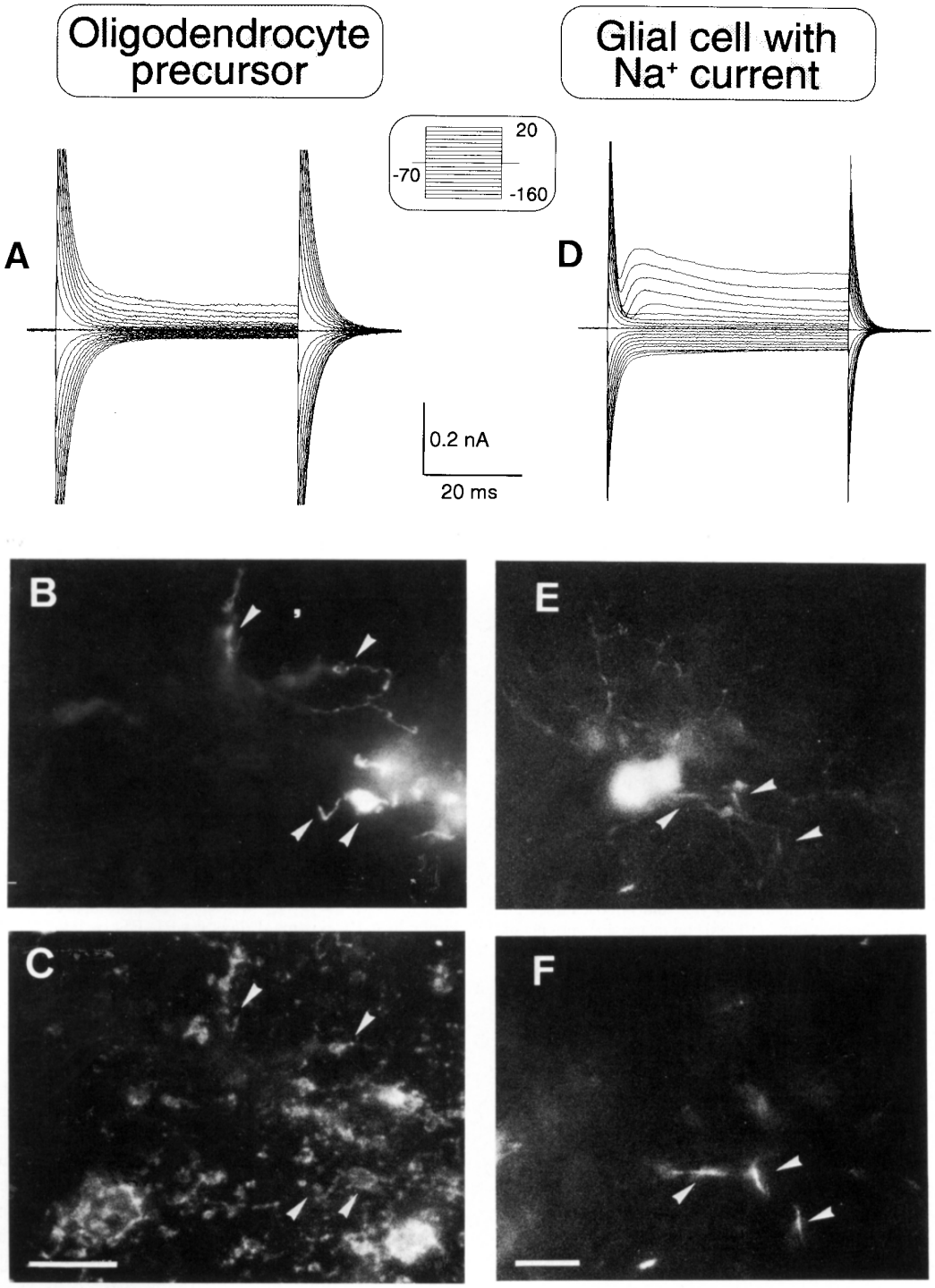

FIG. 5. Membrane current pattern, morphology and immunohistochemistry of oligodendrocyte precursors and of glial cells with Na^+ currents. Membrane currents were recorded with the same protocol as described for Figure 2. (A) Depolarization activated outward currents in this cell from P4. The resting potential was –25 mV. During the recording the cell was filled with Lucifer Yellow as shown in (B). This cell was identified as a cell of the oligodendrocyte lineage by a positive staining for O1/O4 as shown in (C). (D) Another glial cell obtained from P8 responded to depolarization with a fast transient inward current followed by an outward current. The resting potential was –48 mV. The Lucifer Yellow filled cell is depicted in (E). (F) The same cell as in (D) and (E) shows positive staining for GFAP. Scale bars: (B), (C) 10 μm; (E), (D) 10 μm.

Morphological inspection revealed that the somata of these cells were particularly small. Based on the above described features and due to the failure to stain any cell with antibodies for O1/O4 or O4 alone, it is probable that these cells represent a distinct population of astrocytes or astrocyte precursor cells with weak, if any, GFAP expression (Sontheimer and Waxman, 1993).

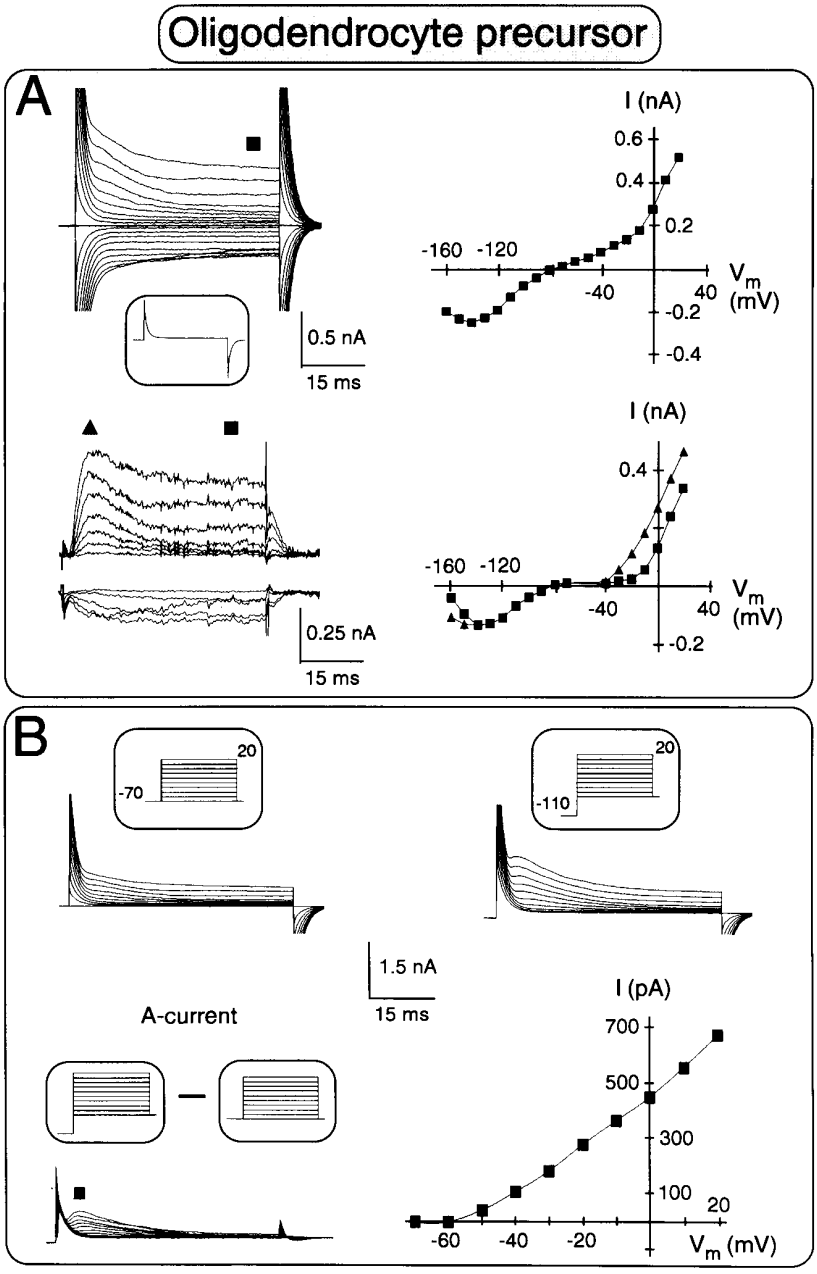

FIG. 6. Membrane properties of oligodendrocyte precursors. (A) Glial cell from P12. Voltage steps were activated as described in the legend to Figure 2 (upper left). The inset shows the response to a depolarization from −70 to −50 mV. This voltage step was used to subtract the time- and voltage-independent current and to isolate the voltage-gated current components (lower left) (for further explanation see text). Current–voltage curves were constructed from the currents shown on the left at the time points indicated by the squares and the triangle. (B) K_A currents in a C-type glial cell. A family of current traces was activated from holding potentials of −70 mV (left upper traces) and −110 mV (right upper traces). The pattern of voltage steps is illustrated in the insets. The K_A current component was isolated by subtracting the family of current traces clamped at −110 mV from that at −70 mV (lower left). Note that the K_A current is partially activated at a holding potential of −70 mV. The peak of these currents was used to construct the current–voltage curve as shown on the right. Currents were measured at the time indicated by the square. Recordings were performed from a cell at P10.

Oligodendrocytes were characterized by passive decaying currents similar to those described for oligodendrocytes of the corpus callosum (Berger *et al.*, 1991). Indeed, we could identify these cells as cells of the oligodendrocyte lineage since many of them were stained against O1/O4, markers for this cell population (Sommer and Schachner, 1981), but not against GFAP. These cells had long processes oriented mainly in parallel, which is typical for oligodendrocytes but in contrast to precursor cells (Butt and Ransom, 1989; Berger *et al.*, 1991).

The channel pattern of the cells with voltage-gated K^+ channels but no Na^+ channels had similarities to late oligodendrocyte precursor cells as described in the corpus callosum slice (Berger *et al.*, 1991). Indeed, some of the cells were positively identified with O1/O4 or O4 alone antibodies, which label oligodendrocytes and late glial precursor cells.

TABLE 1. Membrane currents and immunocytochemical profile of glial cells in the spinal cord

	Astrocyte	Oligodendrocyte	Oligodendrocyte precursor	Glial cell with Na^+-current
K_P	++	++	–	–
K_{DR}	–	–	++	++
K_{IR}	–	–	++	+
K_A	–	–	++	++
Na_V	–	–	–	++
GFAP	+	–	–	+
O1/O4	–	+	+	–
O4	n.d.	n.d.	+	–

The glial cells were classified as astrocytes, oligodendrocytes, oligodendrocyte precursors and glial cells with Na^+ currents according to their channel pattern, immunohistochemistry and morphology. K_P, time-independent, passive K^+ current; Na_V, voltage-activated Na^+ current; ++, detectable in all cells; –, not detectable; +, detectable in a subpopulation of cells; n.d., not determined.

Comparison of glial currents in slices and culture

The passive non-decaying K^+ currents in astrocytes are similar to recordings obtained from astrocytes in hippocampal slices (Steinhäuser *et al.*, 1994). In culture, Sontheimer and co-workers have described Na^+ currents in astrocytes from spinal cord (Sontheimer *et al.*, 1992; Black *et al.*, 1993) and from hippocampal slice (Sontheimer and Waxman, 1993). They have also observed that co-culturing astrocytes with neurons leads to a disappearance of the Na^+ currents (Thio *et al.*, 1993). Thus the presence of the neuronal population in the intact spinal cord may lead to the down-regulation of the Na^+ currents in astrocytes. The cells with Na^+ currents may be astrocyte precursor cells or just at the transition to an astrocyte. This could explain the low probability of GFAP staining in this cell population. The oligodendrocytes had passive decaying currents similar to those described in the corpus callosum slice (Berger *et al.*, 1991; Syková *et al.*, 1994). The decay of the current was attributed

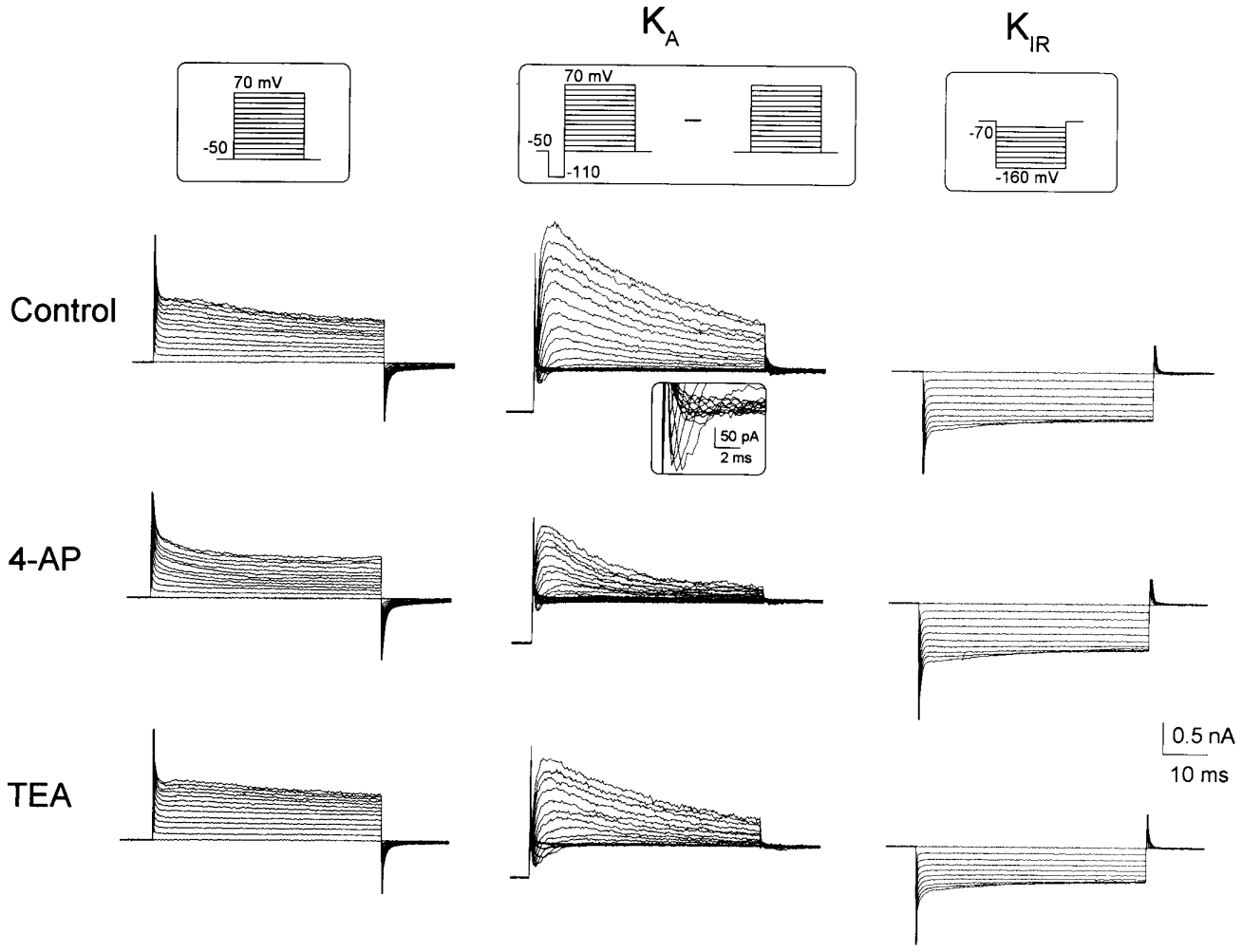

FIG. 7. Pharmacology of glial cells with Na^+ current. The K^+-channel blockers 4-aminopyridine (4-AP, 5 mM) and tetraethylammonium chloride (TEA, 50 mM) were extracellularly applied while recording membrane currents from a glial cell with Na^+ current from P7. The resting potential was –75 mV. To discriminate between the different K^+ currents, protocols of voltage steps were used as indicated in the insets on top of each column. To better distinguish between the K^+ outward currents, the membrane was clamped at –50 mV; this potential is not negative enough to activate Na^+ currents. Therefore the (Na^+) inward currents are enlarged in the inset in the middle. Left column, K_{DR} and passive K^+ currents; middle column, K_A; right column, K_{IR}. The effect of 4-AP (middle row) and TEA (bottom row) in comparison with control conditions (upper row) are shown for each protocol. 4-AP and TEA mainly block the K_A current.

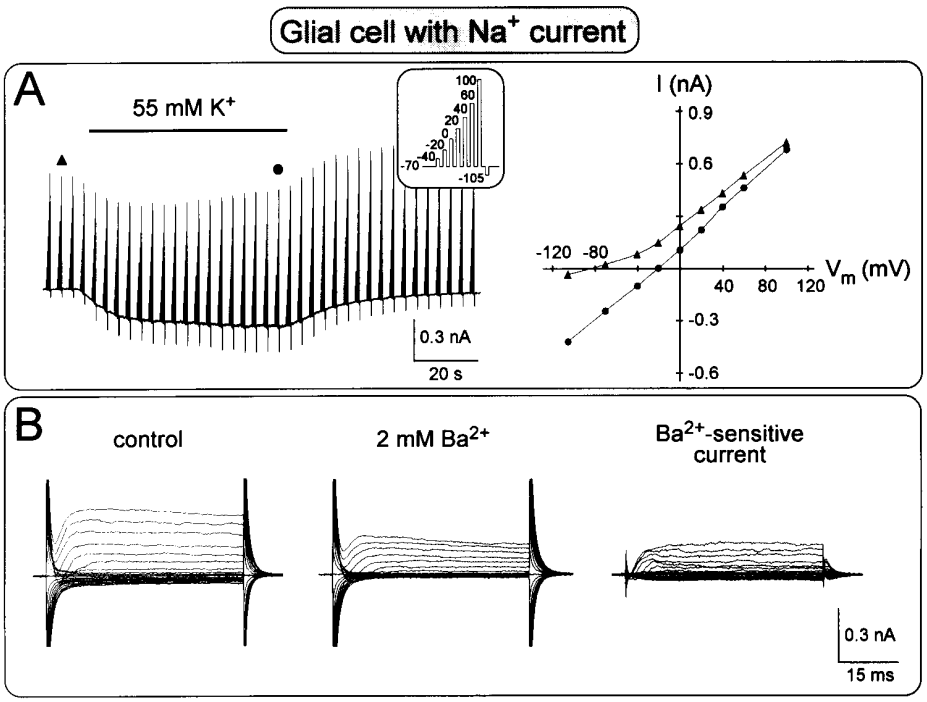

FIG. 8. K^+ current properties of a glial cell with Na^+ current. (A) A glial cell with a Na^+ current from P5 was clamped at –70 mV and subsequently stepped for a series of voltage jumps to de- and hyperpolarizing potentials as indicated in the inset. This voltage clamp protocol was applied repeatedly every 3.7 s. $[K^+]$ in the bathing solution was increased from the control level (5 mM) to 55 mM, as indicated by the bar. From two series of voltage steps in normal (triangles) and elevated $[K^+]$ (circles) current/voltage curves were constructed and are shown on the right. The reversal potential in normal $[K^+]$ was at about –85 mV and in elevated $[K^+]$ (55 mM) at –20 mV. The membrane conductance determined from 0 to +40 mV increased from 2.9 to 5 ns. (B) A glial cell with Na^+ current from P6. Currents were activated by de- and hyperpolarizing voltage steps as described in the legend to Figure 1 in control solution, and after application of 2 mM Ba^{2+}. By subtracting the currents in the presence of Ba^{2+} from the currents in the control solution, the Ba^{2+}-sensitive current was isolated and is shown on the right.

in the latter study to a transmembrane shift of potassium caused by the polarizing voltage jump. The large tail currents observed after the depolarizing and hyperpolarizing voltage jumps reflect the redistribution of the normal K^+ gradient. The tail currents are distinct from capacitative currents since they could be blocked by Ba^{2+}. Berger and co-workers concluded that K^+ is trapped in the narrow extracellular space surrounding the oligodendrocytes when the membrane is de- or hyperpolarized (Berger *et al.*, 1991; Syková *et al.*, 1994). On the other hand, it becomes evident that this feature is characteristic for oligodendrocytes (in contrast to astrocytes and glial precursor cells) and that it can only be observed in slice preparations but not in cell culture (Sontheimer and Kettenmann, 1988; Sontheimer *et al.*, 1989). The current decay (and presumably the degree of K^+ concentration increase in the extracellular space) was less pronounced in this study of the spinal grey matter than in the white matter oligodendrocytes in the corpus callosum. This is in line with the finding that the astrocytes and oligodendrocytes in grey as well as in white matter, in spinal cord, in cerebral cortex and in corpus callosum are surrounded by a larger extracellular space early in development at P1–P15 (Lehmenkühler *et al.*, 1993; Syková and Chvátal, 1993). The finding that oligodendrocytes, but not astrocytes, showed these distinct tail currents suggests that their extracellular microenvironment might be different.

The cells termed precursor cells had many properties in common with late glial precursor cells from the corpus callosum slice, including the presence of the K_{DR} and K_A currents and the lack of Na^+ currents (Berger *et al.*, 1991). In contrast to the late glial precursor cells from the corpus callosum, 79% of the cells from the spinal cord showed a K_{IR} current. In cell cultures from the mouse cortex such a channel pattern was described for the transition stage between precursor cells and oligodendrocytes (Blankenfeld *et al.*, 1992).

The cells with Na^+, K_{DR}, K_A and K_{IR} channels also had many similarities with glial precursor cells recorded in slices of the corpus callosum obtained from early postnatal mice (Berger *et al.*, 1991). Voltage-gated currents were also recorded in a population of glial cells in hippocampal slices (Steinhäuser *et al.*, 1992) and in immunocytochemically identified astrocytes (Sontheimer and Waxman, 1993). Early precursor cells in the corpus callosum express Ca^{2+} channels (Berger *et al.*, 1992a); in the present study we have not used the isolation techniques to detect the Ca^{2+} currents and we thus cannot exclude the possibility that Ca^{2+} channels are present in our cells.

Glial precursor cells with K_{IR} channels had a significantly higher resting membrane potential. This further supports the importance of K_{IR} for the maintenance of a highly negative membrane potential in glial cells as proposed by Barres (1991).

Development changes of channel patterns

In the corpus callosum of the mouse almost all cells at a given age of the animal had a uniform current pattern (Berger *et al.*, 1991). Cells obtained from slices at P3–P4 showed properties of early precursor cells characterized by Na^+, Ca^{2+} and K_{DR} currents (Berger

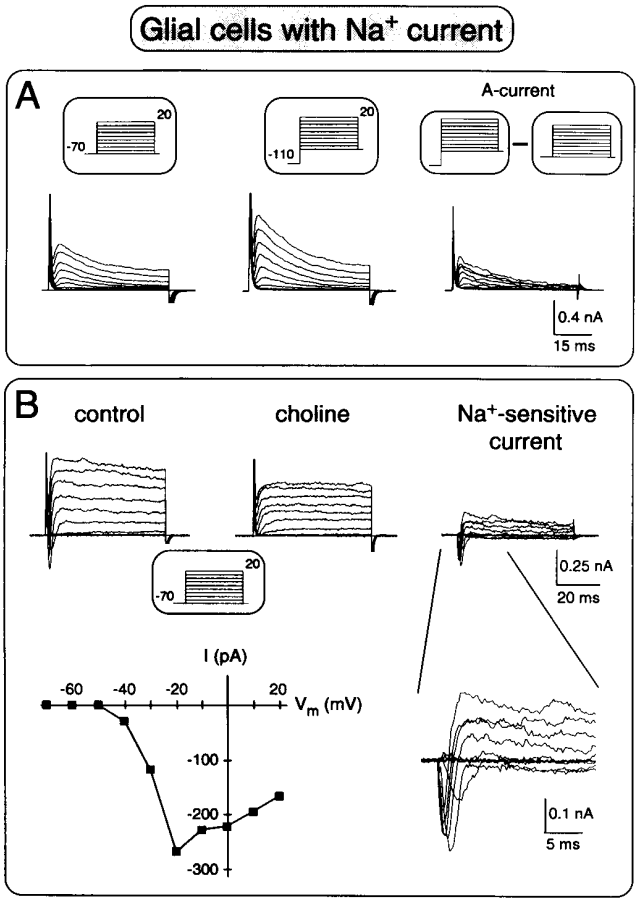

FIG. 9. Na^+ and K_A current properties of a glial cell with Na^+ current. (A) The K_A current component was isolated as described in the legend to Figure 6B. Recordings were performed from a cell at P4. (B) A family of current traces was activated in standard solution (upper left), as shown in the inset, and compared with recordings in a solution where Na^+ was replaced by choline (upper middle). The Na^+-sensitive current (upper right) was isolated by subtracting the currents in choline from control currents. The inward current is shown in an expanded time and current scale on the lower left. A current–voltage curve was constructed from the peak of the inward currents, and is depicted on the lower right. Recordings were performed from a cell at P11.

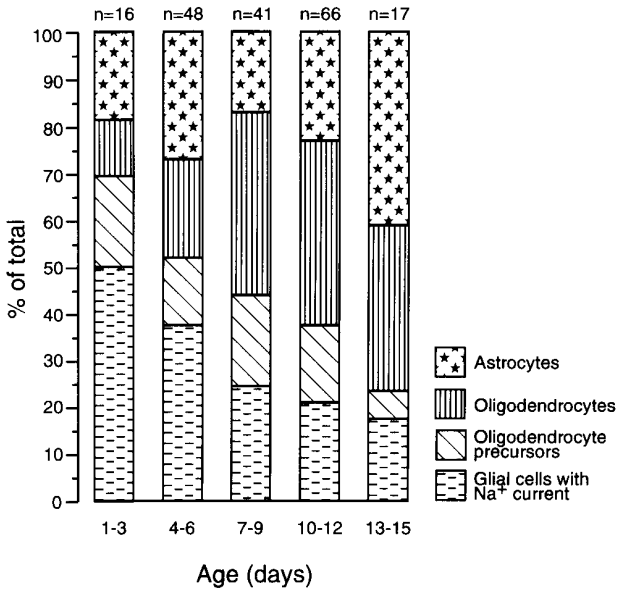

FIG. 10. Relative frequency of recording from the glial cell types. The relative distribution (% of total) of the four different types of glial cells of rat spinal cord is shown for the different age groups of animals from P1 to P15. Data are compiled for several postnatal days, as indicated. The number of cells of each age group is indicated on top of the columns. Recordings were taken from small cells without selecting for particular morphologies.

et al., 1991, 1992a). In slices from 6- to 8-day-old mice most of the cells were still characterized by K_{DR} currents and rarely showed Na^+ currents. In contrast, cells from slices at P10 and older had properties of oligodendrocytes, i.e. passive decaying currents. Thus the developmental regulation of the glial channel pattern in corpus callosum is highly synchronized. In contrast, in the spinal cord grey matter such a synchronized change of immature to mature cell types was not observed. We found all cell types in spinal cord slices obtained from rats between P1 and P19. There was, however, a substantial relative increase in the number of immunohistochemically as well as electrophysiologically identified astrocytes and oligodendrocytes, and a relative decrease of presumable precursor cells during development (Fig. 10). All four cell types were found randomly in all regions of the spinal cord grey matter. The relative frequency of recording from the different types of glial cells might be influenced by the selection and the skill of the experimenter, since cells are selected under visual control. Our findings are, however, in accordance with results of immunohistochemical stainings in the rat spinal cord from P4 to P14 reported by Hirano and Goldman (1988).

Developmental changes of glial cell types and of the extracellular space

Glial cells control the extracellular K^+ homeostasis by spatial buffer currents (Orkand *et al.*, 1966). A prerequisite for these currents is a high K^+ selectivity of the membrane and the formation of a large syncytium. During development, this regulatory mechanism starts to operate from P9 to P11 concomitantly with an increase in GFAP staining of the astrocytes' processes (Jendelová and Syková, 1991; Syková *et al.*, 1992). We have observed that the relative number of astrocytes in the spinal cord increases during that developmental period. The GFAP-labelled cells were usually not coupled to other cells. This is in line with the finding that immature astrocytes do not couple (Fischer and Kettenmann, 1985), and it is likely that coupling among spinal cord astrocytes appears later in development as observed in the rat visual cortex (Binmöller and Müller, 1992).

Regulatory mechanisms, such as the control of the K^+ homeostasis and the regulation of extracellular pH, are performed by the glial cells and are well developed in adult animals. In the young animals used in our present study, these mechanisms are not yet fully functioning (Jendelová and Syková, 1991) since the astrocyte syncytium is not yet developed. Indeed, spinal cord K^+ homeostasis was impaired after uncoupling glial cells (Syková *et al.*, 1988). In young animals the ion fluctuations might be sufficiently buffered by the larger extracellular space and therefore glial uptake may not be required. In spinal cord grey matter the decrease of the extracellular space volume fraction during development is even later than in cortex (Lehmenkühler *et al.*, 1993). In the spinal cord at P5 the values of the extracellular space volume fraction are almost double, and at P12 the values are still larger than in adult animals (Svoboda and Syková,

1991; Syková and Chvátal, 1993). Thus the functional differentiation of spinal cord glial cells may occur in two steps. First, the number of astrocytes and oligodendrocytes gradually increases while the relative number of glial precursor cells decreases from P1 to P15. At P9–P12 the extracellular space volume fraction has decreased to 50% of the volume at P5 (Syková and Chvátal, 1993) and glial cells start to control ionic (K^+ and pH) homeostasis in the spinal cord (Jendelová and Syková, 1991; Syková *et al.*, 1992). In older animals the extracellular space further decreases and astrocytes form an extensive syncytium to maintain ion homeostasis over a larger spatial range. These results suggest that the functional properties of glial cells are adapted to the needs of the developing and adult CNS.

Acknowledgements

We thank Regina Krauss for excellent technical assistance and Marianne Frankowski for help with the micrographs. This work was supported by the Deutsche Forschungsgemeinschaft (SFB 317), by the Bundesministerium für Forschung und Technologie and by the Grant Agency of the Czech Republic (Grant no. 309/93/1048).

Abbreviations

4-AP	4-aminopyridine
GFAP	glial fibrillary acidic protein
K_A	A-type K^+
K_{DR}	delayed rectifying K^+
K_{IR}	inwardly rectifying K^+
O	markers of the oligodendrocytic lineage
P	postnatal day
TEA	tetraethylammonium chloride

References

Barres, B. A. (1991) New roles for glia. *J. Neurosci.*, **11**, 3685–3694.

Barres, B. A., Chun, L. L. Y. and Corey, D. P. (1988) Ion channel expression by white matter glia: type 2 astrocytes and oligodendrocytes. *Glia*, **1**, 10–30.

Barres, B. A., Chun, L. L. Y. and Corey, D. P. (1990a) Ion channels in vertebrate glia. *Annu. Rev. Neurosci.*, **13**, 441–474.

Barres, B. A., Koroshetz, W. J., Chun, L. L. Y. and Corey, D. P. (1990b) Ion channel expression by white matter glia: the type-1 astrocyte. *Neuron*, **5**, 527–544.

Berger, T., Schnitzer, J. and Kettenmann, H. (1991) Developmental changes in the membrane current pattern, K^+ buffer capacity and morphology of glial cells in the corpus callosum slice. *J. Neurosci.*, **11**, 3008–3024.

Berger, T., Schnitzer, J., Orkand, P. M. and Kettenmann, H. (1992a) Sodium and calcium currents in glial cells of the mouse corpus callosum slice. *Eur. J. Neurosci.*, **4**, 1271–1284.

Berger, T., Walz, W., Schnitzer, J. and Kettenmann, H. (1992b) GABA and glutamate activate currents in glial cells of the corpus callosum slice. *J. Neurosci. Res.*, **31**, 21–27.

Binmöller, E. J. and Müller, C. M. (1992) Postnatal development of dye-coupling among astrocytes in rat visual cortex. *Glia*, **6**, 127–137.

Black, J. A., Sontheimer, H. and Waxman, S. G. (1993) Spinal cord astrocytes *in vitro*: phenotypic diversity and sodium channel immunoreactivity. *Glia*, **7**, 272–285.

Blankenfeld, G. V., Verkhratzky, A. N. and Kettenmann, H. (1992) Calcium channels in the oligodendrocyte lineage. *Eur. J. Neurosci.*, **4**, 1035–1048.

Butt, A. M. and Ransom, B. R. (1989) Visualization of oligodendrocytes and astrocytes in the intact rat optic nerve by intracellular injection of Lucifer Yellow and horseradish peroxidase. *Glia*, **2**, 470–475.

Chesler, M. (1990) The regulation and modulation of pH in nervous system. *Prog. Neurobiol.*, **34**, 401–427.

Connor, J. A. and Stevens, C. F. (1971) Voltage clamp studies of a transient outward membrane current in gastropod neural somata. *J. Physiol. (Lond.)*, **213**, 21–30.

Debus, E., Weber, K. and Osborn, M. (1983) Monoclonal antibodies specific for glial fibrillary acidic (GFA) protein and for each of the neurofilament triplet polypeptides. *Differentiation*, **25**, 193–203.

Edwards, F. A., Konnerth, A., Sakmann, B. and Takashaki, T. (1989) A thin slice preparation for patch clamp recordings from neurons of the mammalian central nervous system. *Pflügers Arch.*, **414**, 600–612.

Eng, L. F., Vanderhaegen, J. J., Bignami, A. and Gerstl, B. (1971) An acidic protein isolated from fibrous astrocytes. *Brain Res.*, **28**, 351–354.

Fischer, G. and Kettenmann, H. (1985) Cultured astrocytes form a syncytium after maturation. *Exp. Cell Res.*, **159**, 273–279.

Fischer, G., Leutz, A. and Schachner, M. (1992) Cultivation of immature astrocytes of mouse cerebellum in a serum-free, hormonally defined medium. Appearance of the mature astrocytic phenotype after addition of serum. *Neurosci. Lett.*, **29**, 297–302.

Gilmore, S. A. (1963) The effects of X-irradiation on the spinal cords of neonatal rats. II. Histological observations. *J. Neuropathol. Exp. Neurol.*, **22**, 294–301.

Gilmore, S. A. (1971) Neuroglial population in the spinal white matter of neonatal and early postnatal rats: an autoradiographic study of numbers of neuroglia and changes in their proliferative activity. *Anat. Rec.*, **171**, 283–291.

Hamill, O. P., Marty, E., Neher, E., Sakmann, B. and Sigworth, F. J. (1981) Improved patch clamp techniques for high resolution current recording from cells and cell-free membrane patches. *Pflügers Arch.*, **391**, 85–100.

Hirano, M. and Goldman, J. E. (1988) Gliogenesis in rat spinal cord: evidence for origin of astrocytes and oligodendrocytes from radial precursors. *J. Neurosci. Res.*, **21**, 155–167.

Jendelová, P. and Syková, E. (1991) Role of glia in K^+ and pH homeostasis in the neonatal rat spinal cord. *Glia*, **4**, 56–63.

Kettenmann, H., Orkand, R. K., Lux, H. D. and Schachner, M. (1982) Single potassium channel currents in cultured mouse oligodendrocytes. *Neurosci. Lett.*, **32**, 41–46.

Kettenmann, H., Sonnhof, U. and Schachner, M. (1983) Exclusive potassium dependence of the membrane potential in cultured mouse oligodendrocytes. *J. Neurosci.*, **3**, 500–505.

Kettenmann, H., Sonnhof, U., Camerer, H., Kuhlmann, S., Orkand, R. K. and Schachner, M. (1984) Electrical properties of oligodendrocytes in culture. *Pflügers Arch.*, **401**, 324–332.

Kettenmann, H., Blankenfeld, G. V. and Trotter, J. (1992) Ion channel expression during the development of oligodendrocytes. In Abbott, N. J., Leiberman, E. M. and Raff, M. C. (eds), *Glial–Neuronal Interactions*. New York Academy of Science, New York, pp. 64–77.

Kettenmann, H., Banati, R. and Walz, W. (1993) Electrophysiological behavior of microglia. *Glia*, **7**, 93–101.

Lehmenkühler, A., Syková, E., Svoboda, J., Zilles, J. K. and Nicholson, C. (1993) Extracellular space parameters in the rat neocortex and subcortical white matter during postnatal development determined by diffusion analysis. *Neuroscience*, **55**, 339–351.

Levison, S. V. and Goldman, J. E. (1993) Both oligodendrocytes and astrocytes develop from progenitors in the subventricular zone of postnatal rat forebrain. *Neuron*, **10**, 201–212.

MacVicar, B. A. (1984) Voltage gated Ca^{2+} channels in glial cells. *Science*, **226**, 1345–1347.

Matthews, M. A. and Duncan, D. (1971) A quantitative study of morphological changes accompanying the initiation and process of myelin production in the dorsal funiculus of the rat spinal cord. *J. Comp. Neurol.*, **141**, 1–22.

Orkand, R. K., Nicholls, J. G. and Kuffler, S. W. (1966) The effect of nerve impulse on the membrane potential of glial cells in the central nervous system of amphibia. *J. Neurophysiol.*, **29**, 788–806.

Ritchie, J. M. (1992) Voltage gated ion channels in Schwann cells and glia. *Trends Neurosci.*, **29**, 345–351.

Sandell, J. H. and Masland, R. H. (1988) Photoconversion of some fluorescent markers to a diaminobenzidine product. *J. Histochem. Cytochem.*, **36**, 555–559.

Sims, T. J., Waxman, S. G., Black, J. A. and Gilmore, S. A. (1985) Perinodal astrocytic processes at nodes of Ranvier in developing normal and glial deficient rat spinal cord. *Brain Res.*, **337**, 321–333.

Sommer, I. and Schachner, M. (1981) Monoclonal antibodies (O1 to O4) to oligodendrocyte cell surfaces: an immunocytological study in the central nervous system. *Devl Biol.*, **83**, 311–323.

Sontheimer,H. and Kettenmann, H. (1988) Heterogeneity of potassium currents in cultured oligodendrocytes. *Glia*, **1**, 415–420.

Sontheimer, H. and Waxman, S. G. (1992) Ion channels in spinal cord astrocytes *in vitro*. II. Biophysical and pharmacological analysis of Na^+-currents. *J. Neurophysiol.*, **68**, 1001–1011.

Sontheimer, H. and Waxman, S. G. (1993) Expression of voltage-activated ion channels by astrocytes and oligodendrocytes in the hippocampal slice. *J. Neurophysiol.*, **70**, 1863–1873.

Sontheimer, H., Trotter, J., Schachner, M. and Kettenmann, H. (1989)

Developmental regulation of channel expression in cultured oligodendrocytes. *Neuron*, **2**, 1135–1145.

Sontheimer, H., Black, J. A., Ransom, B. R. and Waxman, S. G. (1992) Ion channels and spinal cord astrocytes *in vitro*. I. Transient expression of high levels of Na^+ and K^+ channels. *J. Neurophysiol.*, **68**, 985–1000.

Steinhäuser, C., Berger, T., Frotscher, M. and Kettenmann, H. (1992) Heterogeneity in the membrane current pattern of identified glial cells in the hippocampal slice. *Eur. J. Neurosci.*, **4**, 472–484.

Steinhäuser, C., Jabs, R. and Kettenmann, H. (1994) L-Glutamate induced inward currents are covered by a simultaneous block of voltage dependent potassium currents in identified hippocampal glial cells of mice. *Hippocampus*, in press.

Svoboda, J. and Syková, E. (1991) Extracellular space volume changes in the rat spinal cord produced by nerve stimulation and peripheral injury. *Brain Res.*, **560**, 216–224.

Syková, E. (1983) Extracellular K^+ accumulation in the central nervous system. *Prog. Biophys. Mol. Biol.*, **42**, 135–189.

Syková, E. (1992) Ionic and volume changes in the microenvironment of nerve and receptor cells. *Prog. Sensory Physiol.*, **13**, 1–167.

Syková, E. and Chvátal, A. (1993) Extracellular ionic and volume changes: the role in glia–neuron interaction. *J. Chem. Neuroanat.*, **6**, 247–260.

Syková, E., Orkand, R. K., Chvátal, A., Hájek,I. and Kríz, N. (1988) Effects of carbon dioxide on extracellular potassium accumulation and volume in isolated frog spinal cord. *Pflügers Arch.*, **412**, 183–187.

Syková, E., Jendelová, P., Šimonová, Z. and Chvátal, A. (1992) K^+ and pH homeostasis in the developing rat spinal cord is impaired by early postnatal X-irradiation. *Brain Res.*, **594**, 19–30.

Syková, E., Berger, T., Chvátal, A., Lehmenkühler, A. and Kettenmann, H. (1994) Changes in properties of glial cell in white matter during postnatal development coincide with the changes in extracellular space volume. *Physiol. Res.*, in press.

Thio, C. L., Waxman, S. G. and Sontheimer, H. (1993) Ion channels in spinal cord astrocytes *in vitro*. III. Modulation of channel expression by coculture with neurons and neuron-conditioned medium. *J. Neurophysiol.*, **69**, 819–831.

Tse, F. W., Fraser, D. D., Duffy, S. and MacVicar, B. A. (1992) Voltage-activated K^+ currents in acutely isolated hippocampal astrocytes. *J. Neurosci.*, **12**, 1781–1788.

Walz, W. (1989) Role of glial cells in the regulation of the brain ion microenvironment. *Prog. Neurobiol.*, **33**, 309–333.